The Abdus Salam
International Centre
for Theoretical Physics

United Nations
Educational, Scientific and
Cultural Organization

IAEA
International Atomic Energy Agency

2356-28

Targeted Training Activity: ENSO-Monsoon in the Current and Future Climate

30 July - 10 August, 2012

The Leading Mode of Intra-seasonal Variability of the South Asian Summer Monsoon

SHUKLA Jagadish

Center For Ocean Land Atmosphere Studies, COLA GMU
Institute For Global Environment and Society, IGES
4041 Powder Mill Road, Suite 302, Calverton 20705-3106 MD
U.S.A.

WALLACE John Michael

University of Washington, Dept. of Atmospheric Sciences
Box 351640
WA 98195-1640 Seattle
U.S.A.

The Leading Mode of Intra-seasonal Variability of the South Asian Summer Monsoon

Ravi P. Shukla[1] and John M. Wallace[2]

1. Centre for Ocean-Land-Atmosphere Studies, Calverton, Maryland

2. Atmospheric Sciences, University of Washington, Seattle, WA

Targeted Training Activity (TTA) on "ENSO Monsoon in the Current and Future Climate" (July 30 - August 10, 2012)

International Centre for Theoretical Physics (ICTP), Trieste, Italy

Ravi P. Shukla and John M. Wallace (Journal of Climate in review, 2012)

Background…

- **During the months of October through May the most important mode of intra-seasonal variability of rainfall and wind over South Asia is the Madden Julian Oscillation (MJO).**
- **From June through August, the intensity of the Asian summer monsoon is modulated by the so-called "monsoon intra-seasonal oscillation (MISO) &**
- **Leading modes of OLR variability are not simple in this case (The dominant pattern of variability, often referred to as the monsoon intraseasonal oscillation)**

- **Singular spectrum analysis (SSA) of OLR over South Asia (Annamalai and Slingo 2001, Krishnamurthy and Shukla 2008)**
- Extended EOF analysis of GPCP rainfall anomalies over India and the adjacent seas (Suhas et al. 2012)
- In composites of bandpass-filtered 850 hPa zonal wind anomalies at a reference point just south of the climatological-mean "monsoon trough" over northern India (Goswami and Mohan 2001)
- In composites of heavy rainfall events over the Bay of Bengal (Hoyos and Webster 2007, Bharath Raj and Sengupta 2012

- ✓ We have intentionally refrained from the use of bandpass filtering, extended EOF analysis or Multi-channel singular spectrum analysis so as to **avoid imposing any constraints on the time scale of the patterns** or **the manner in which they evolve.**

- ✓ We have also **avoided specifying any particular geographical area** of emphasis, as is typically done in compositing.

- ✓ In this sense, our analysis serves to **bridge the gap** between prior studies that have been based on contrasting analysis methodologies.

Data

---) The principal data set used in this study **is daily grid point outgoing longwave radiation (OLR)** data on a 2.5° × 2.5° grid derived from NOAA polar orbiting satellites for the period.

---) Tropical Rainfall Measuring Mission (TRMM) rainfall: 0.25° x 0.25°

---) Daily APHRODITE rainfall data set over land: 0.50° x 0.50°

---) Daily wind, geopotential height and sea level pressure data with 2.5°x 2.5° resolution were obtained from the NCEP-NCAR reanalysis dataset

---) The daily sea surface temperature (SST) data are the NOAA optimum interpolation 1/4 degree daily SST

---) The all-season real-time multivariate MJO index (RMM1 and RMM2)

---) The cold tongue index (CTI: Deser and Wallace 1990) that is used to represent the ENSO-related variability

The cold tongue index: The cold tongue index (CTI) is the average SST anomaly over 6N-6S, 180-90W minus the global mean SST

--) **Pentad anomalies** (**obtained by subtracting the respective seasonal-varying climatological-mean fields from total field**)

--) **EOFs analysis was performed on the:-**

(**OLR field and on the 850 and 150 hPa wind fields**)

defined within a:-

(number of different domains)

comprising South Asia during the monsoon season (JJAS)

--) **Most of the results shown in this lecture will base on:-**

(The leading EOFs of OLR defined within the domain **57.5°E – 180°E, 22.5°S – 40°N**)

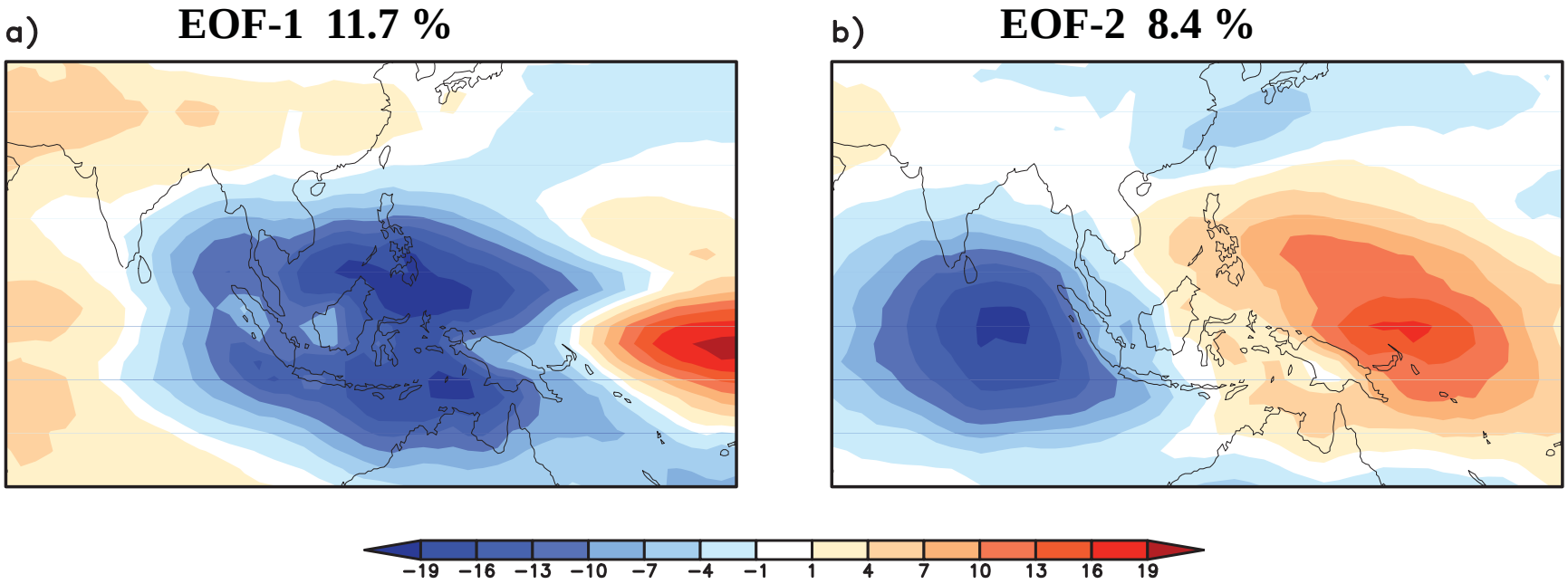

Leading EOFs (OLR based on pentad-mean data (October-May)

EOF1 mode (mostly characterized by a single convection center near the maritime continent)

EOF2 mode (east-west dipole structure with enhanced convection over the eastern Indian Ocean and suppressed convective activities over the tropical western Pacific.

EOF2 (East – West dipole pattern, indication of eastward phase propagation)

MCA Domain

OLR pentad-mean data (October to May)

(57.5^0 E – 180^0 E, 22.5^0 S - 40^0 N)

d/dt (OLR) (October to May)

Where, d/dt is defined to a centered 2-pentad difference

(57.5^0 E – 180^0 E, 22.5^0 S - 40^0 N)

Ravi P. Shukla and John M. Wallace, Journal of Climate in review (2012)

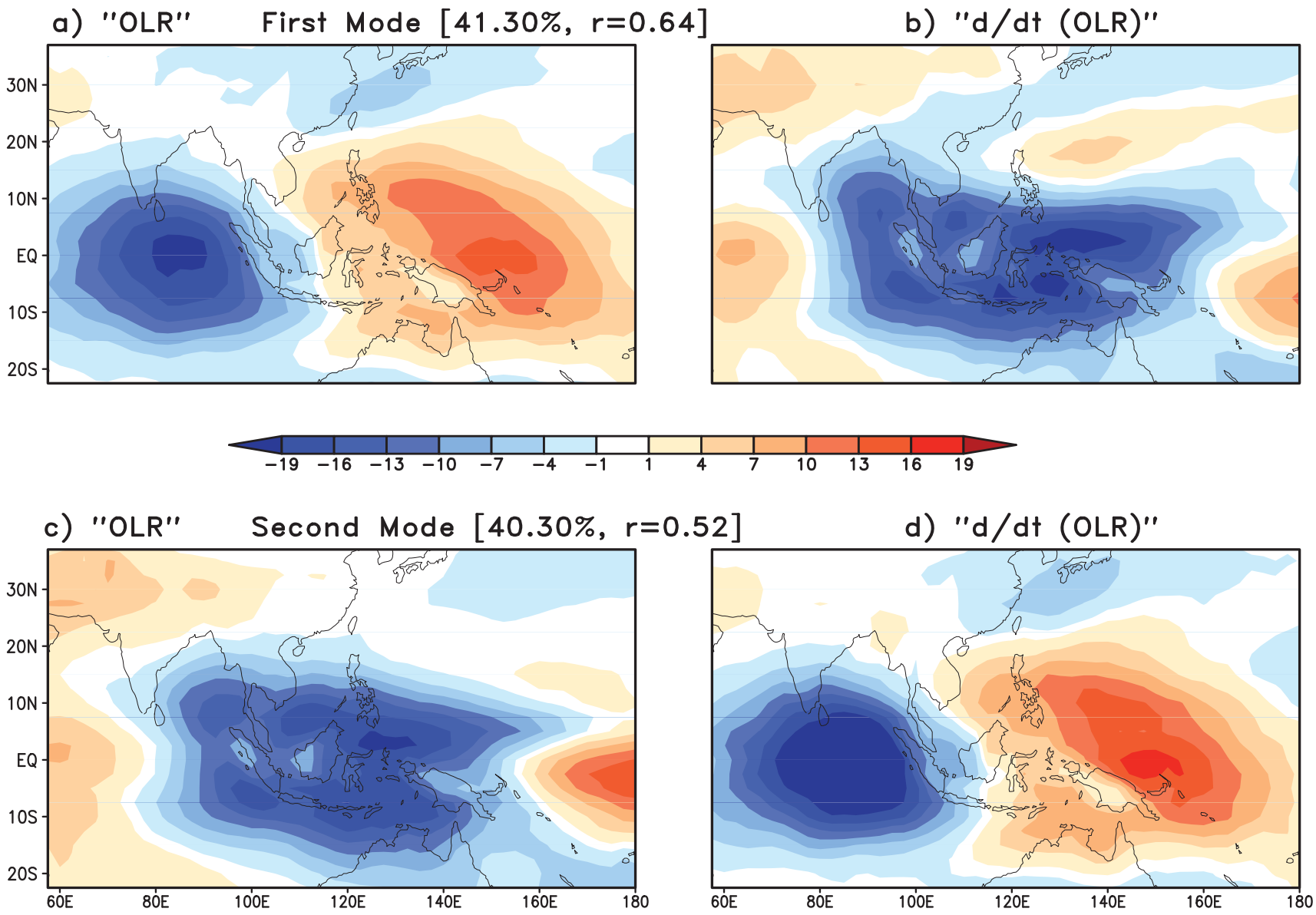
a) "OLR" First Mode [41.30%, r=0.64]
b) "d/dt (OLR)"
30N
20N
10N
EQ
10S
20S
−19 −16 −13 −10 −7 −4 −1 1 4 7 10 13 16 19
c) "OLR" Second Mode [40.30%, r=0.52]
d) "d/dt (OLR)"
60E 80E 100E 120E 140E 160E 180

Main Points:

1) Spatial structure of the MISO as represented in OLR, TRMM rainfall data and the APHRODITE dataset based on station data over land.

2) Analysis of the wind and geo-potential height patterns associated with the MISO in both the lower troposphere and the upper troposphere.

3) MISO signature in the sea surface temperature field.

4) Analysis of the interrelation between the MISO and the MJO.

5) Correspondence between the MISO and active and break spells of the Indian summer monsoon.

a) **OLR and Wind850hPA**

b) **TRMM rainfall**

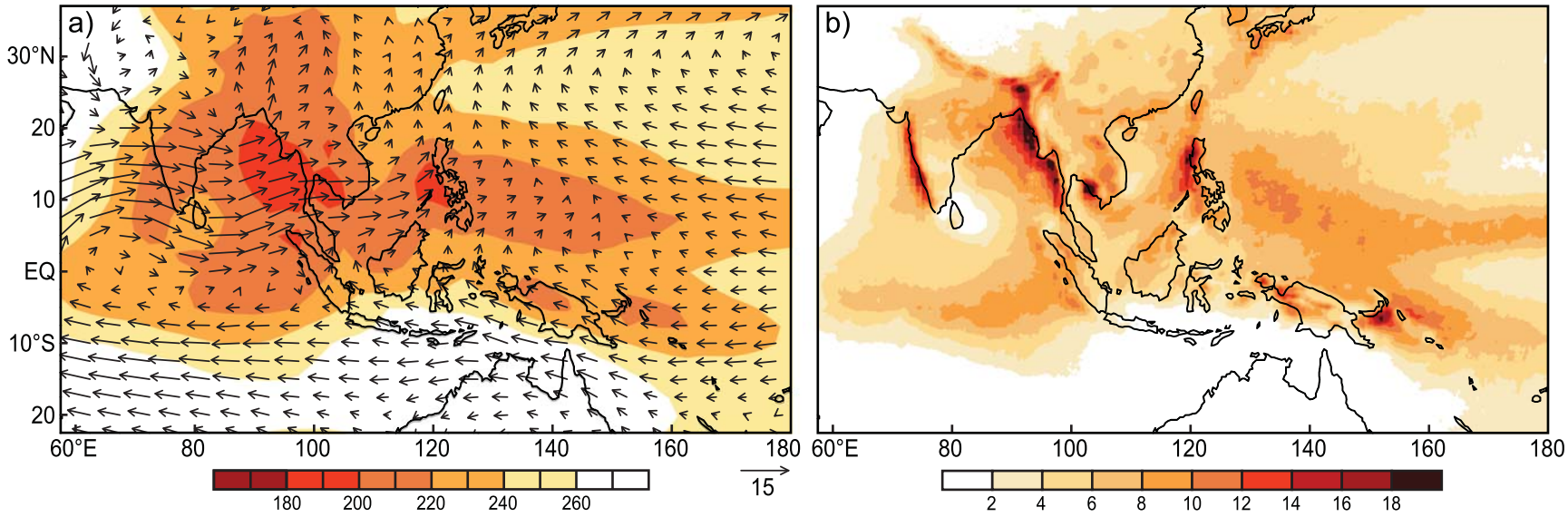

The JJAS OLR and 850 hPa wind climatologies and the corresponding TRMM rainfall climatology

The Asian summer monsoon corresponds:

(**The band of low OLR and enhanced TRMM rainfall**: Include most of the Indian Ocean and land &

(**Hint of a separation** between northern and southern branches across the sector that corresponds to the Bay of Bengal)

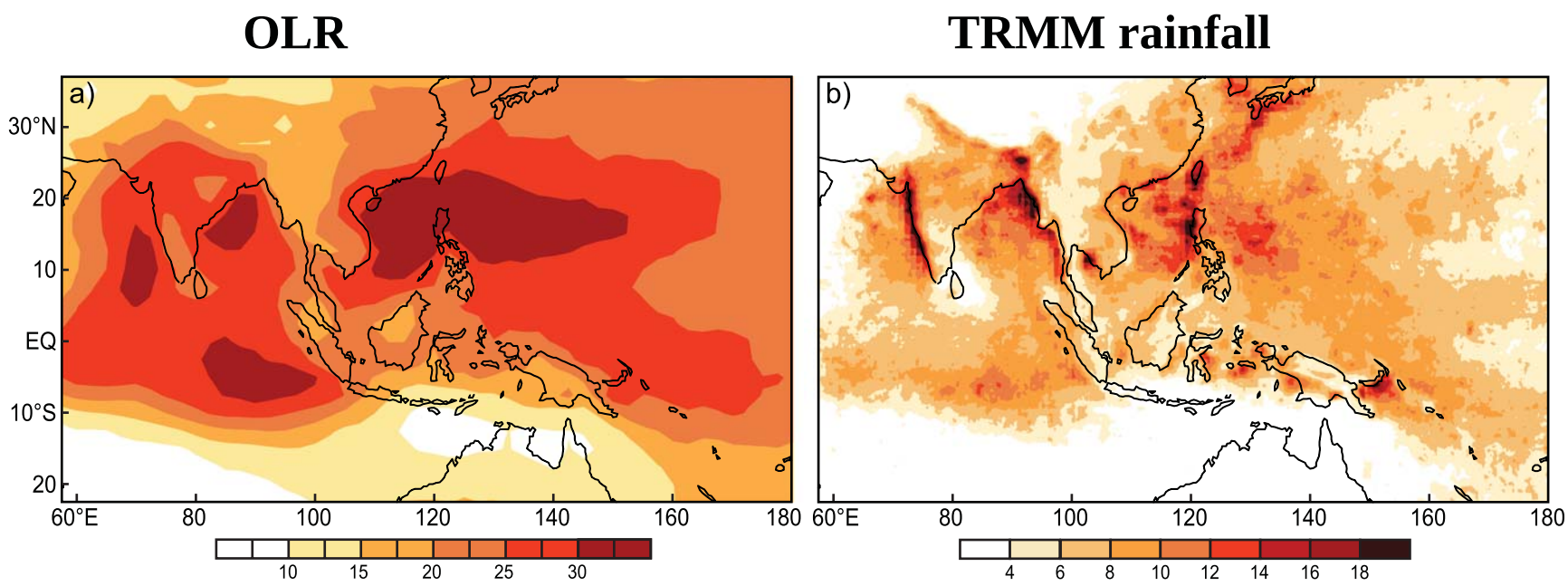

Standard deviation of pentad-mean (*a*) OLR in units of W m^{-2} and (*b*) TRMM rainfall in mm d^{-1}.

Over most of the region (the standard deviation of the OLR data is rather uniform)

TRMM rainfall data (exhibit enhanced variability in the regions of enhanced rainfall)

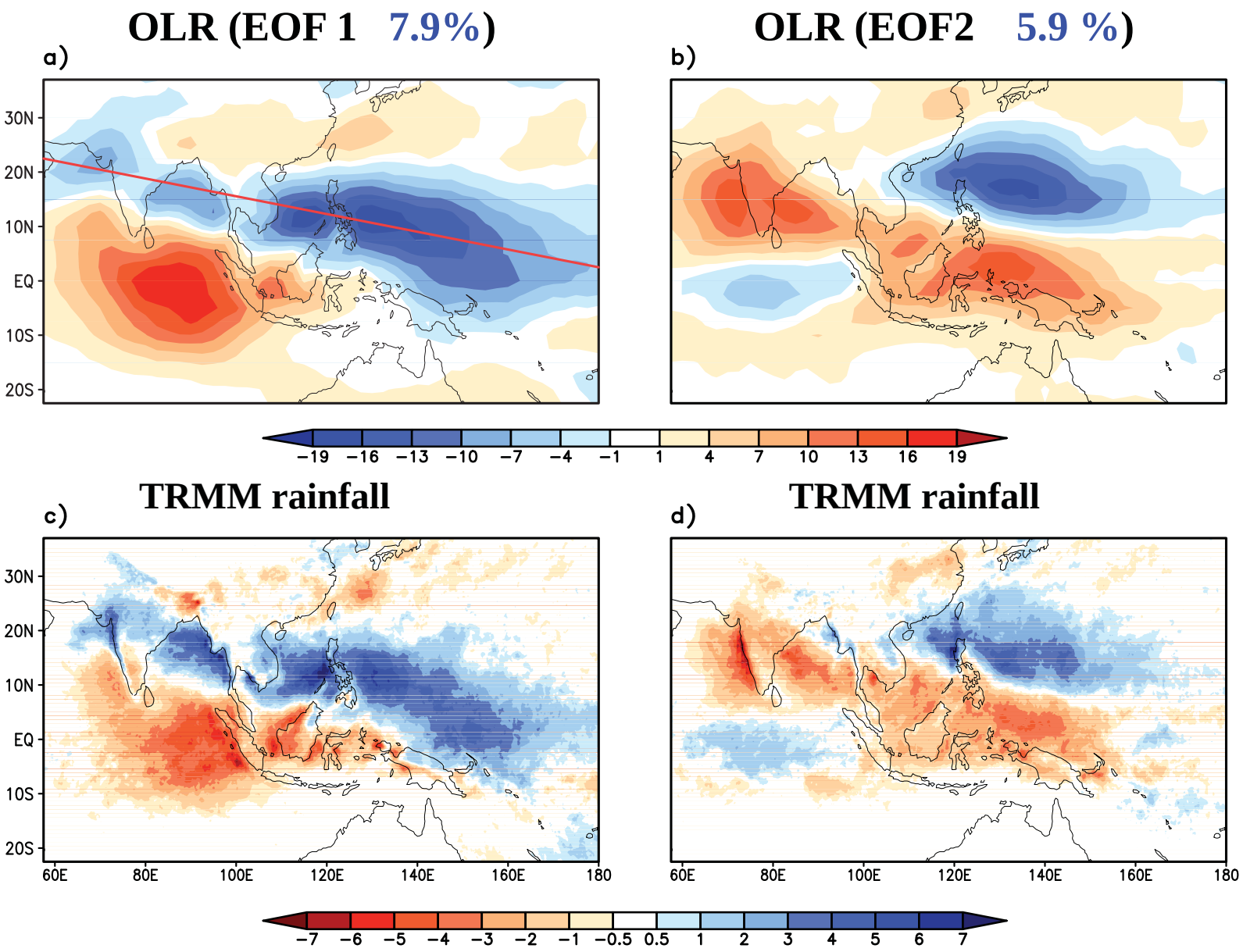
OLR (EOF 1 7.9%)
OLR (EOF2 5.9 %)
a)
b)
30N
20N
10N
EQ
10S
20S
−19 −16 −13 −10 −7 −4 −1 1 4 7 10 13 16 19
TRMM rainfall
TRMM rainfall
c)
d)
60E 80E 100E 120E 140E 160E 180
−7 −6 −5 −4 −3 −2 −1 −0.5 0.5 1 2 3 4 5 6 7

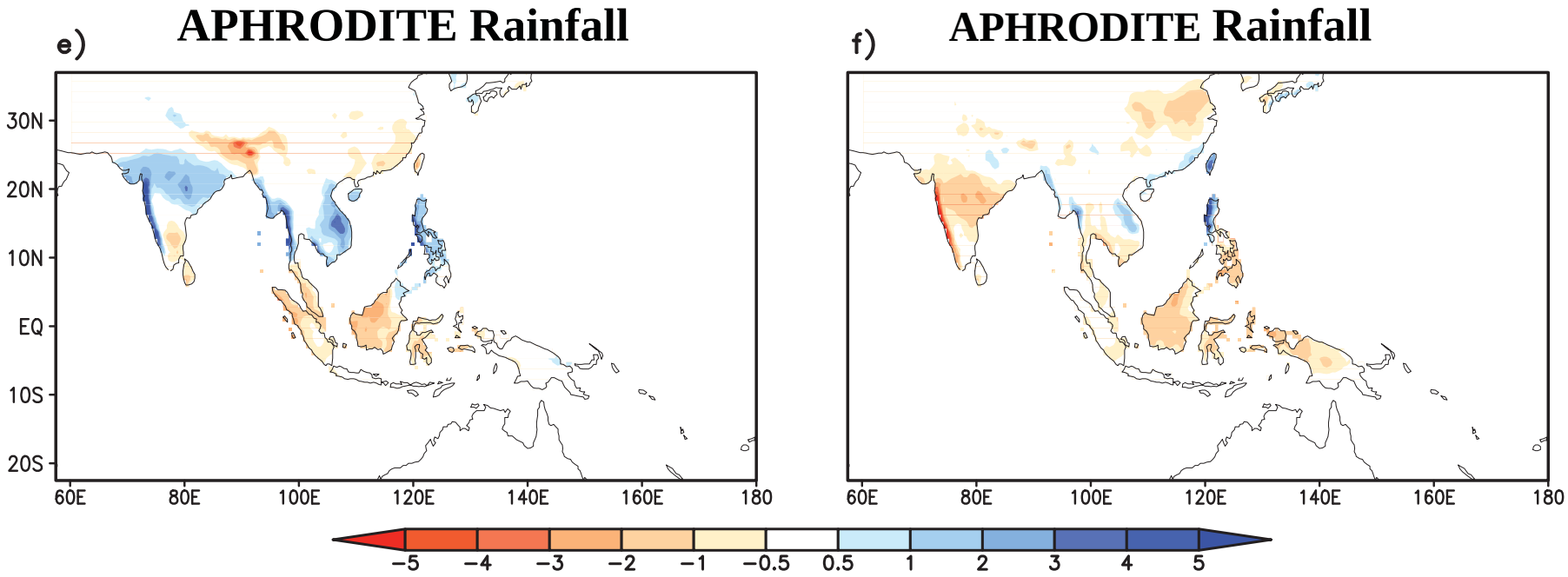

Pentad JJAS APHRODITE rainfall field regressed on standardized PC1 and PC2 of OLR.

----) The corresponding patterns in rainfall over land (generally consistent with the patterns in OLR and TRMM rainfall data)

Correlation coefficient between PC-1,2 of OLR and OLR, TRMM rainfall, Rainfall

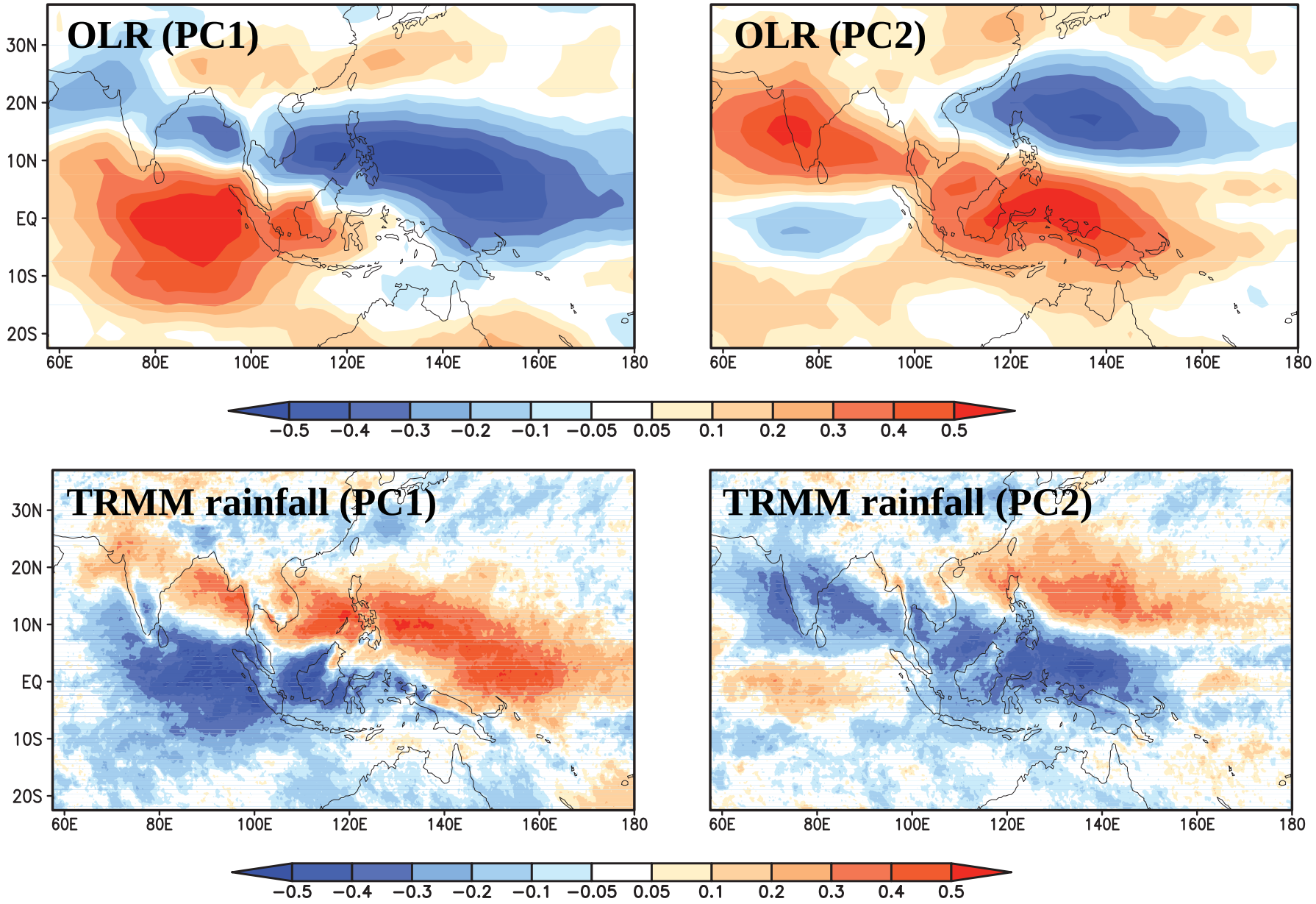

Rainfall (PC1)

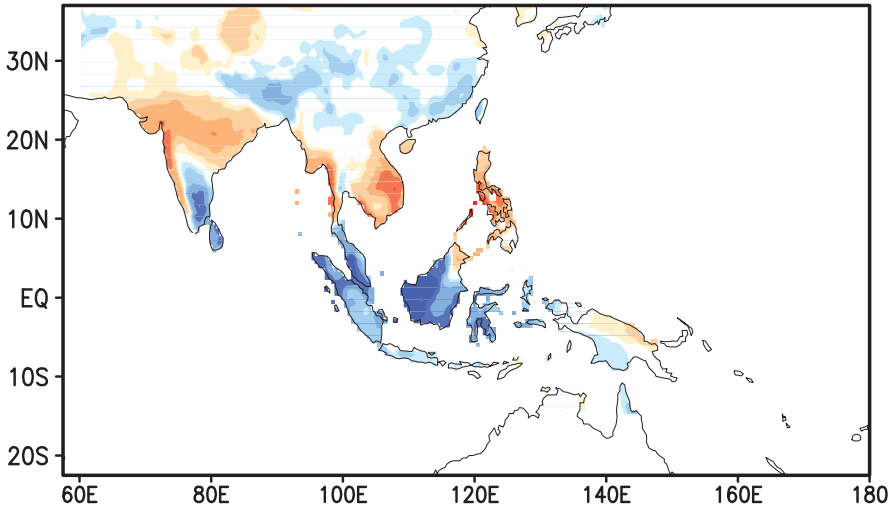

Rainfall (PC2)

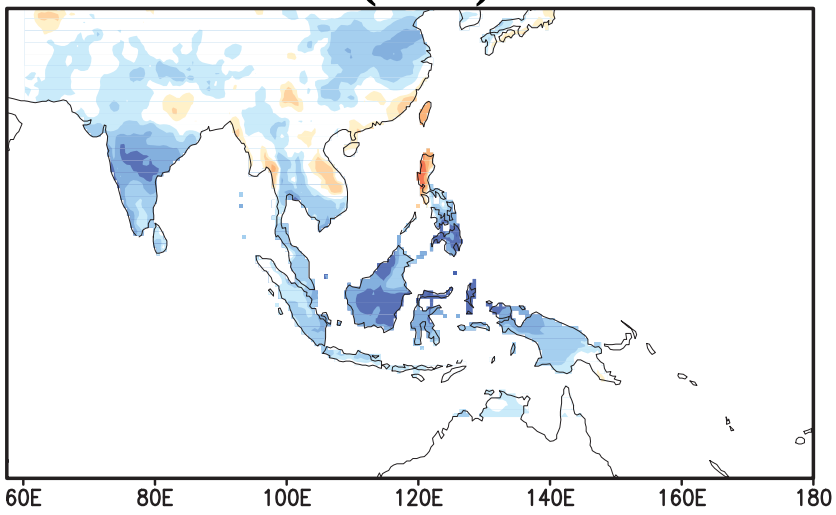

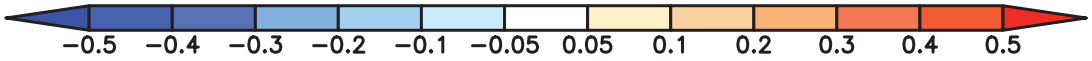

Correlation coefficients at most of the dominant centers of action are on order of three or more times this reference value (95%) (Student t statistic)

Correlation coefficient between the cold tongue index (CTI) and PC3 of OLR is **0.87**

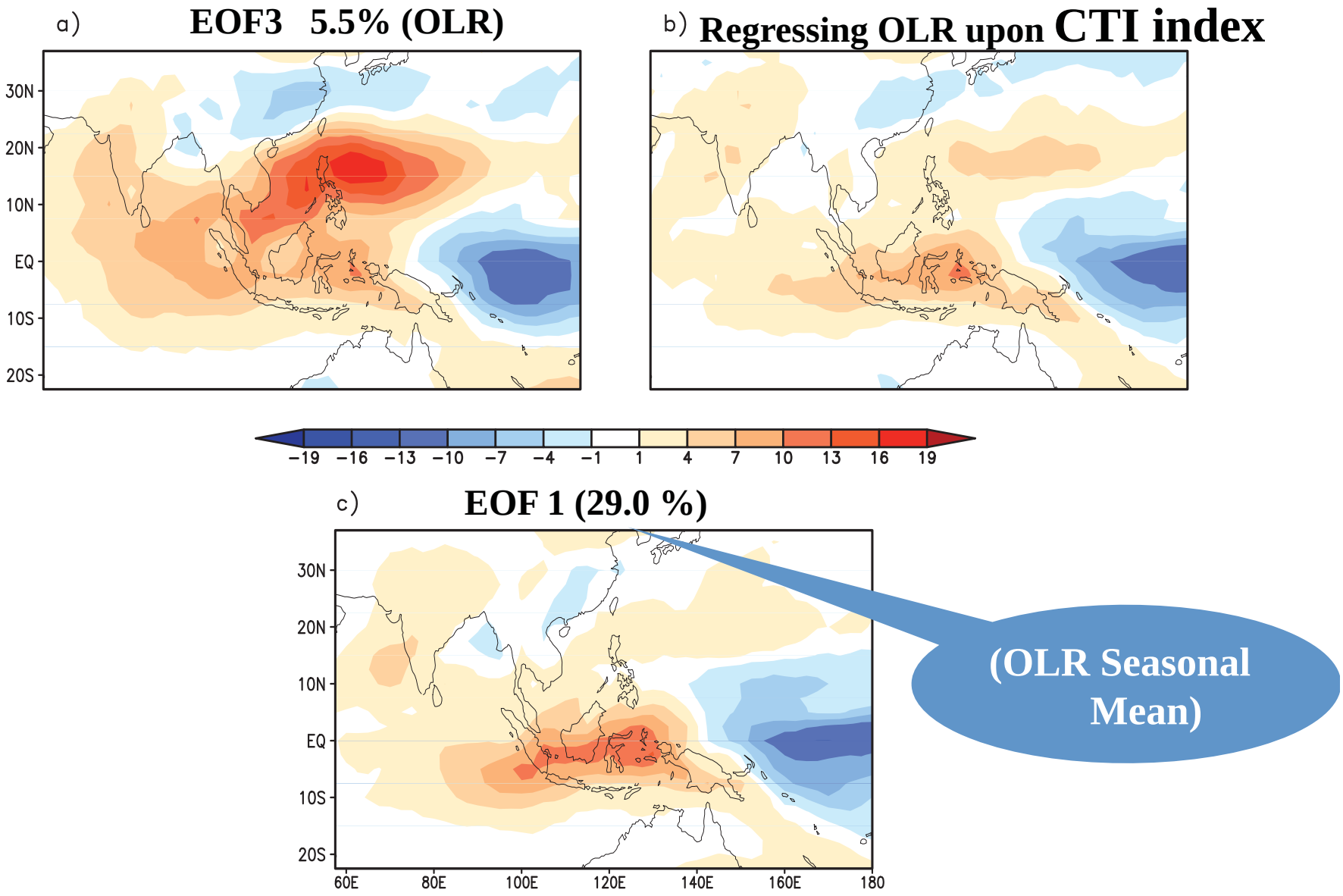

Krishnamurthy and Shukla (2008) obtained a similar "interannual mode" in their singular spectrum analysis

Cross-correlation between the two leading principal components (A lag of +1 indicates PC1 leading PC2 by 1 pentad)										
-5	**-4**	**-3**	**-2**	**-1**	**0**	**1**	**2**	**3**	**4**	**5**
0.05	-0.02	–0.15	–0.30	–0.31	0.00	0.38	0.52	0.42	0.19	0.02
Cross Correlation (PC-1 & PC-2) (+ve PCs value)										
0.03	0.00	-0.05	-0.14	-0.17	-0.01	0.19	0.26	0.22	0.11	0.03
Cross Correlation (PC-1 & PC-2 (-ve PCs value)										
0.02	-0.02	-0.09	-0.16	-0.14	0.01	0.19	0.26	0.20	0.07	-0.01

Evolution of the leading patterns of intraseasonal variability

1) Second mode being displaced northward relative to those in the leading mode.

2) There is a tendency for the pattern of the EOF1 to evolve into pattern of EOF2 over the course of ~ 2 pentad.

3) The **correlation is stronger** for **PC2 lagging PC1** than **PC1 lagging PC2**

4) EOF1 ----> EOF 2 (more coherent) than EOF2 ------> -EOF1

5) RMM1 and RMM2 are widely used to describe the **evolution of the MJO**, PC1 and PC2 can used to describe the evolution of the MISO (cross-correlation (0.49): RMM2 lagging RMM1 by 2 pentad)

4 panel figures :) **Z1) PC1 Z2) PC1+PC2 Z3) PC2 Z4) –PC1 + PC2**

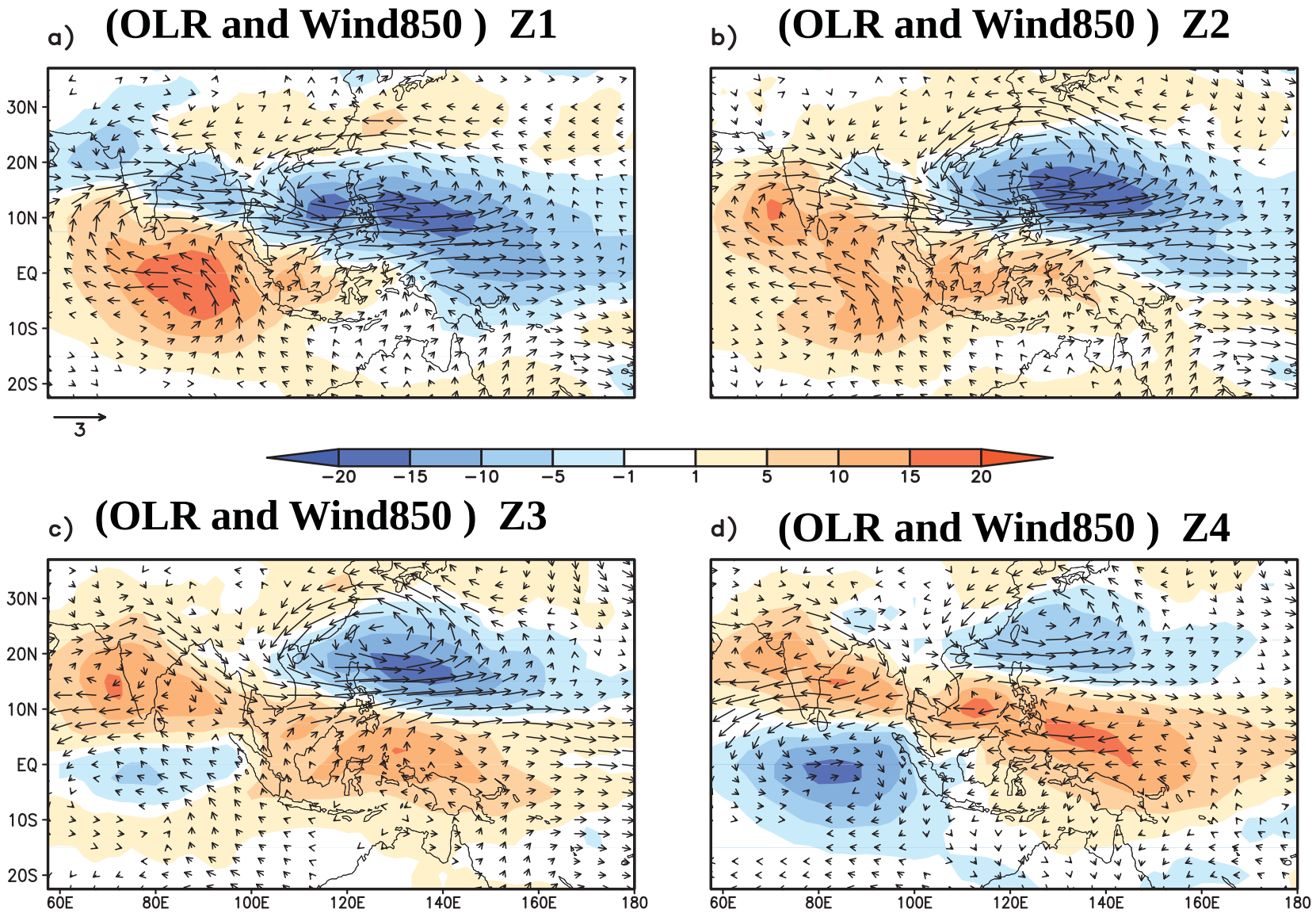
a) (OLR and Wind850) Z1
b) (OLR and Wind850) Z2
c) (OLR and Wind850) Z3
d) (OLR and Wind850) Z4
30N
20N
10N
EQ
10S
20S
3
−20
−15
−10
−5
−1
1
5
10
15
20
60E
80E
100E
120E
140E
160E
180

MCA Domain

OLR pentad-mean data (JJAS)

(57.5^0 E – 180^0 E, 22.5^0 S - 40^0 N)

d/dt (OLR) (JJAS)

Where, d/dt is defined to a centered 2-pentad difference

(57.5^0 E – 180^0 E, 22.5^0 S - 40^0 N)

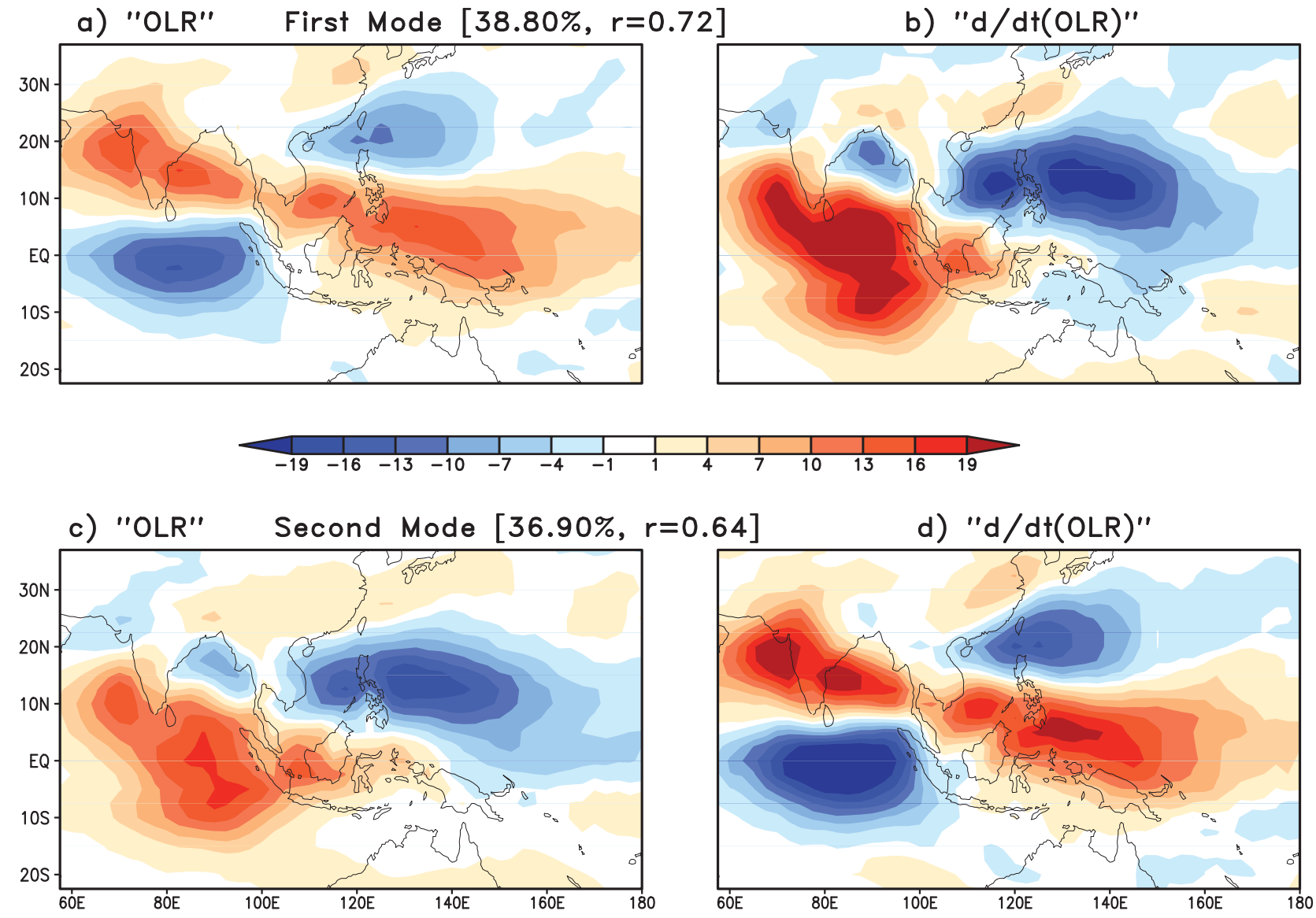

GrADS: COLA/IGES

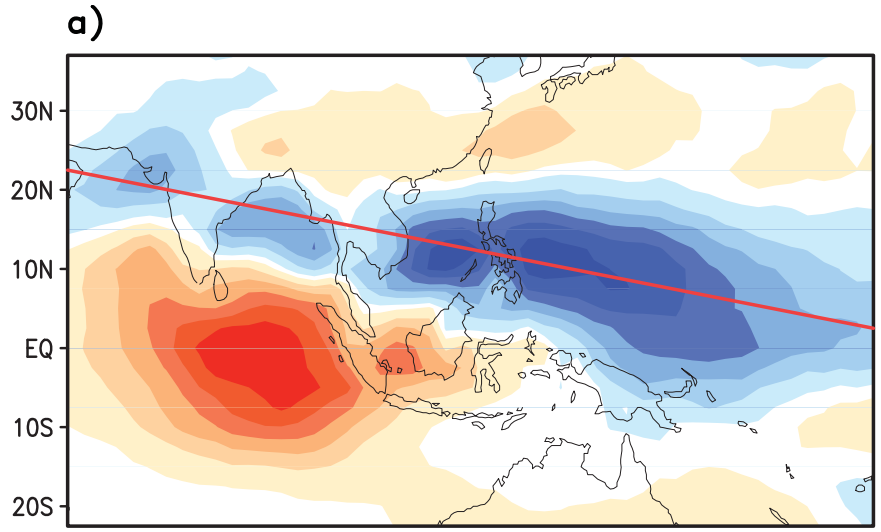

---) For further evidence of the northward propagation

(time-latitude plots of zonally averaged OLR and TRMM rainfall) **based on daily data.**

---) The zonal averaging is performed relative to the sloping line

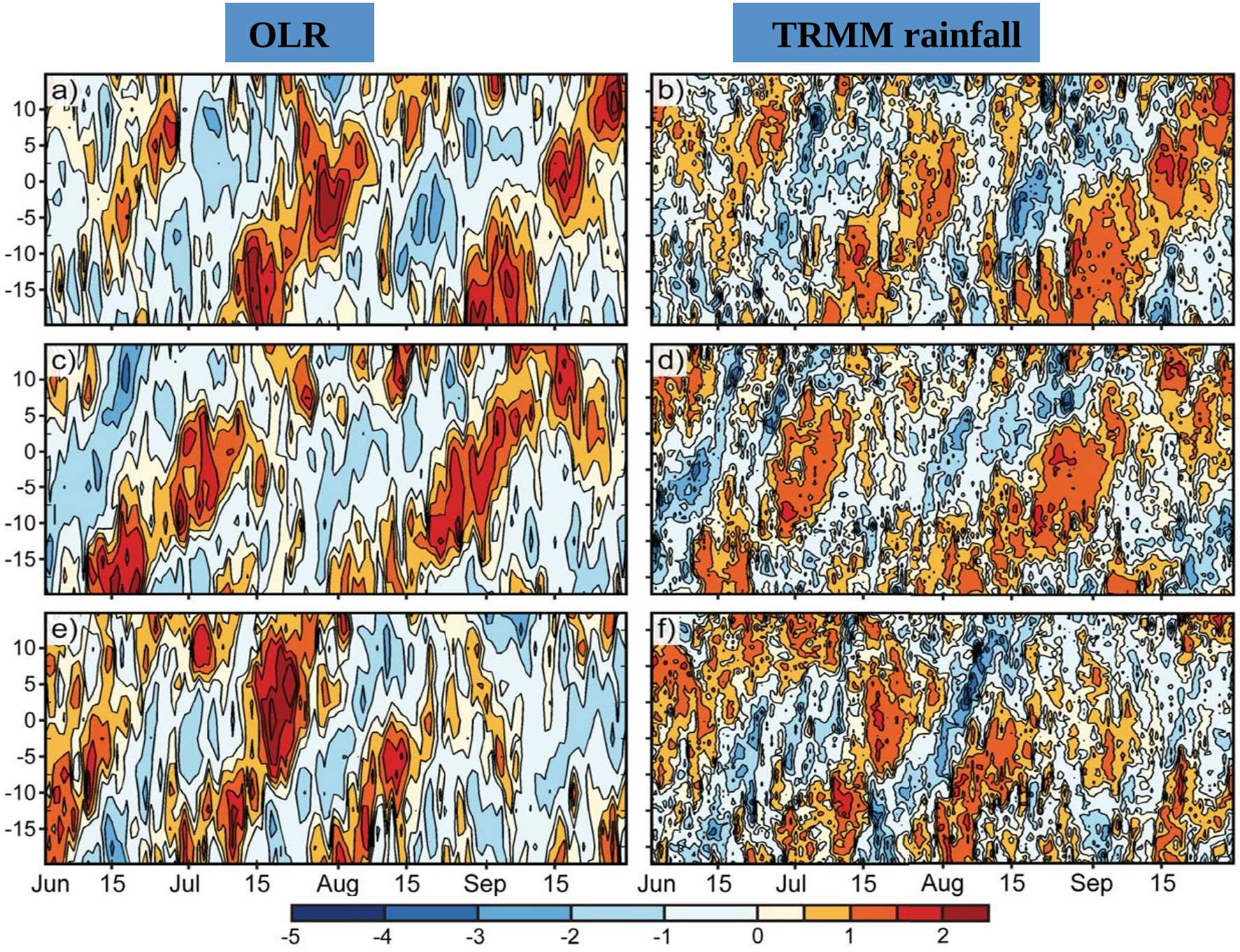
OLR
TRMM rainfall
a)
b)
c)
d)
e)
f)
10
5
0
-5
-10
-15
Jun
15
Jul
15
Aug
15
Sep
15
-5
-4
-3
-2
-1
0
1
2

Standardized meridional profiles of a selection of variables relative to the sloping reference line

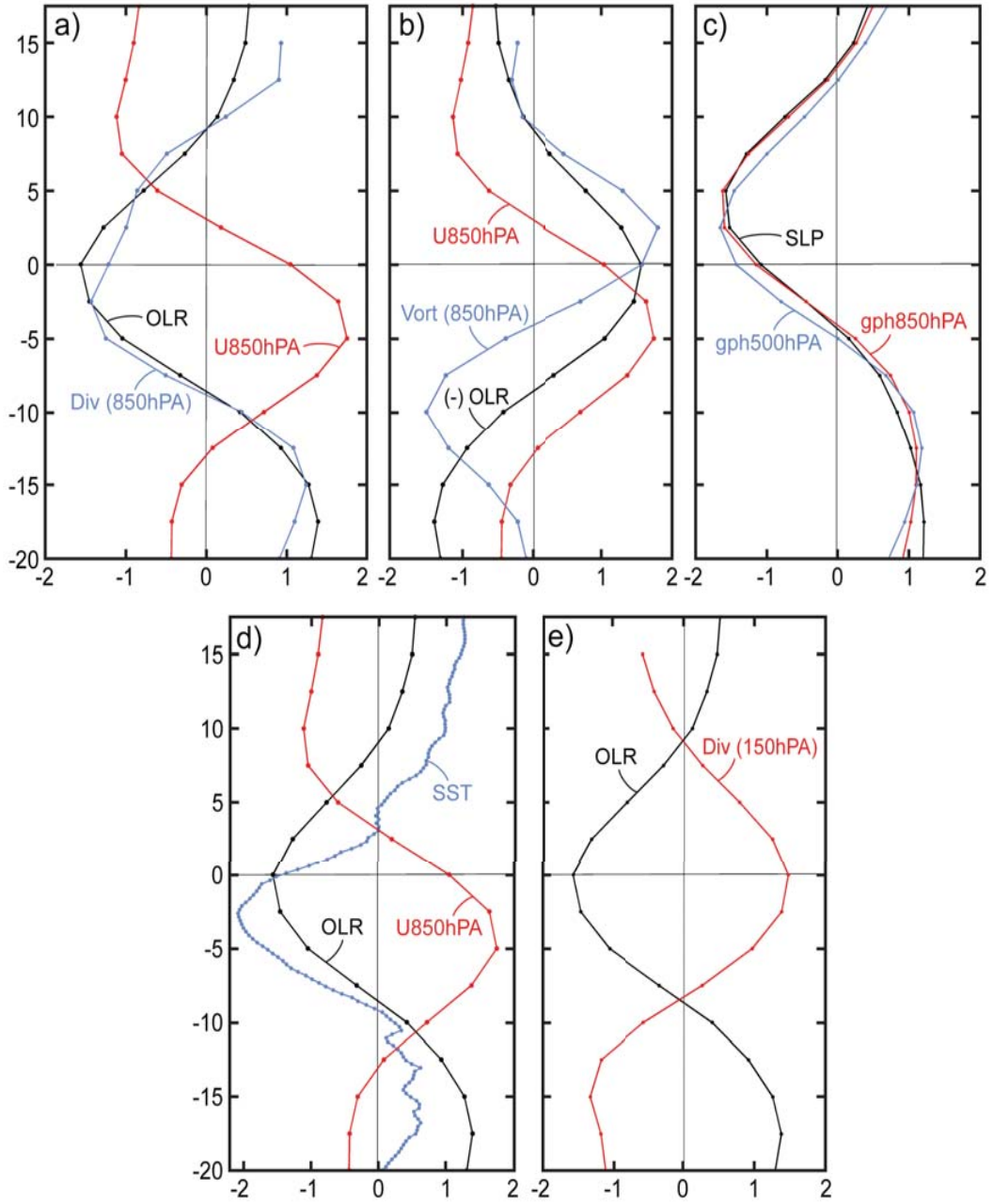

Fig. (a)

① The divergence profile is similar to the OLR profile and also peaks at the reference latitude.

② The strongest westerly wind anomalies are located two grid points (5 degrees of latitude) to the south of the reference latitude

Fig. (b)

① While the strongest cyclonic vorticity anomalies are located one grid point (2.5 degrees of latitude) to the north of it

Fig. (c)

① The SLP profiles and the 850, 700, and 500 hPa height profiles shown in Fig.*c* are similar and almost in phase

Fig. (d)

① SST (Fig. *d*) is lowest 2.5° of latitude to the south of the minimum OLR and 2.5° to the north of the strongest westerly wind anomalies

Fig. (e)

① At the 150 hPa level the meridional profile of divergence is closely aligned with the OLR profile

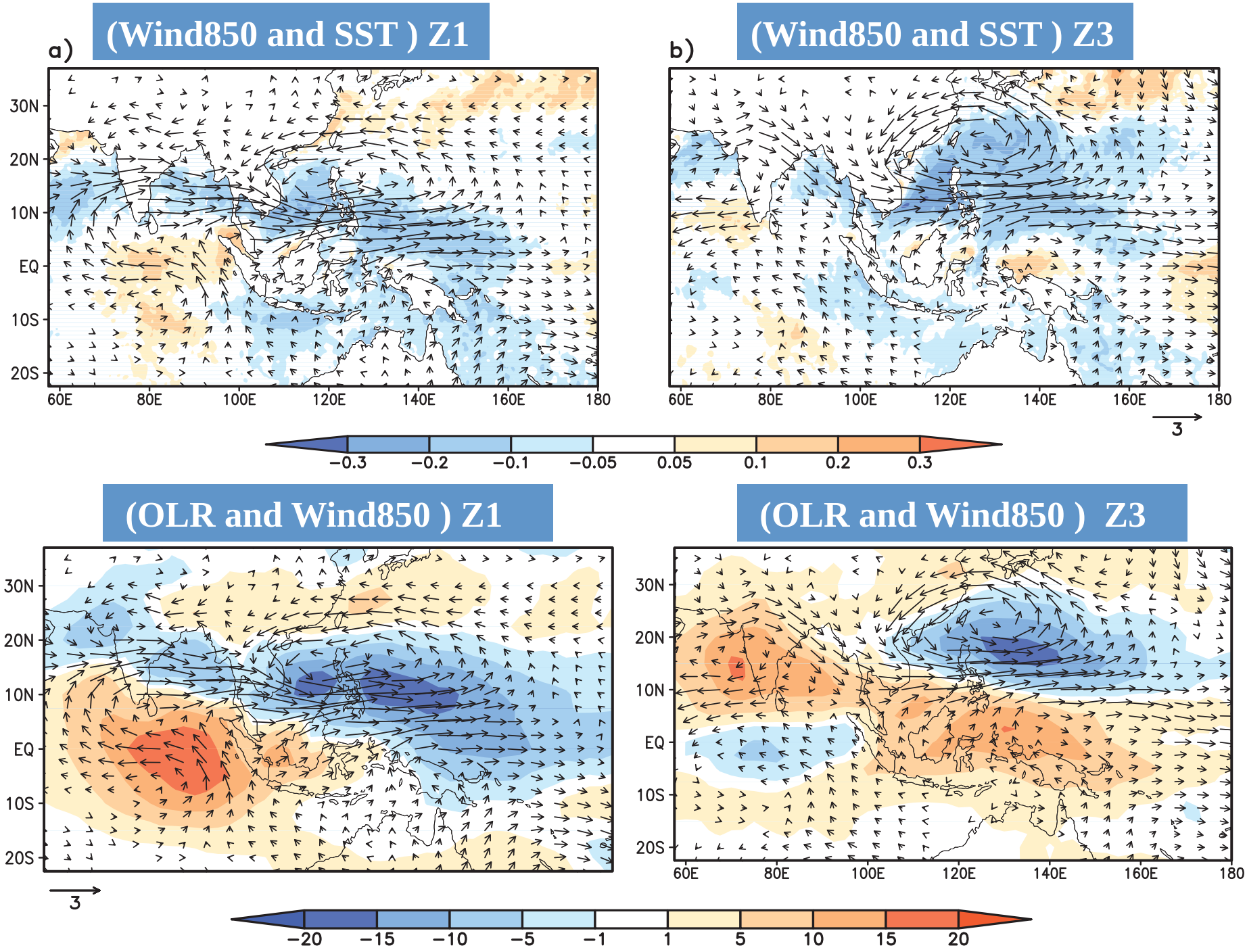
(Wind850 and SST) Z1
a)
(Wind850 and SST) Z3
b)
30N
20N
10N
EQ
10S
20S
60E
80E
100E
120E
140E
160E
180
3
−0.3
−0.2
−0.1
−0.05
0.05
0.1
0.2
0.3
(OLR and Wind850) Z1
(OLR and Wind850) Z3
−20
−15
−10
−5
−1
1
5
10
15
20

Relation between MISO and the year-round MJO

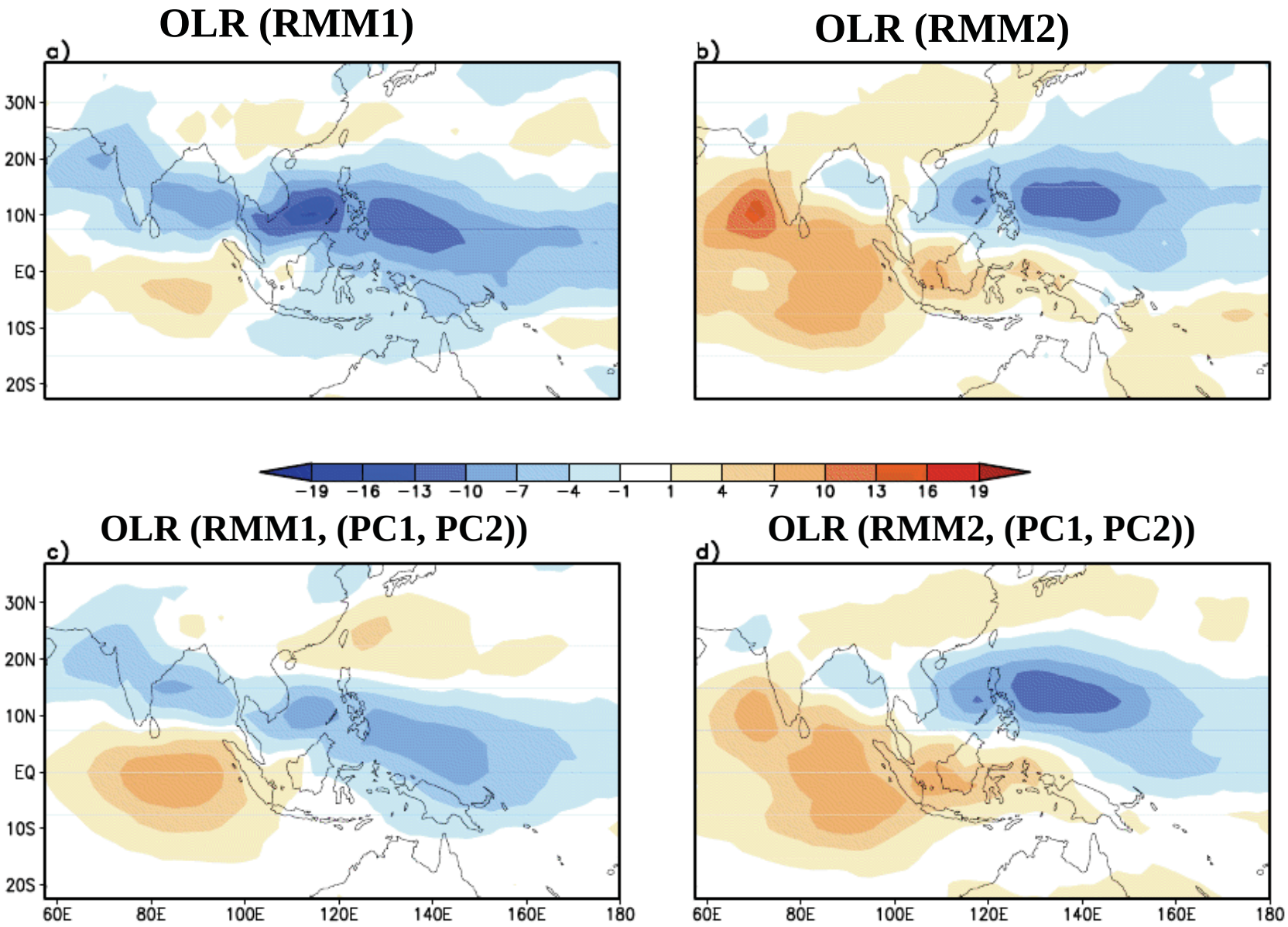

Impact of the MISO on the Asian summer monsoon

- The MISO-related perturbations are large enough to reorganize distributions of rainfall, OLR and wind in the Asian summer monsoon on a time scale of weeks.

- Most dramatic in this respect are the changes associated with fluctuations in PC1.

- For example, in the case of OLR, the composites were constructed by adding and subtracting the field shown in EOF1 (OLR) multiplied by 1.5 from the JJAS climatology of OLR field.

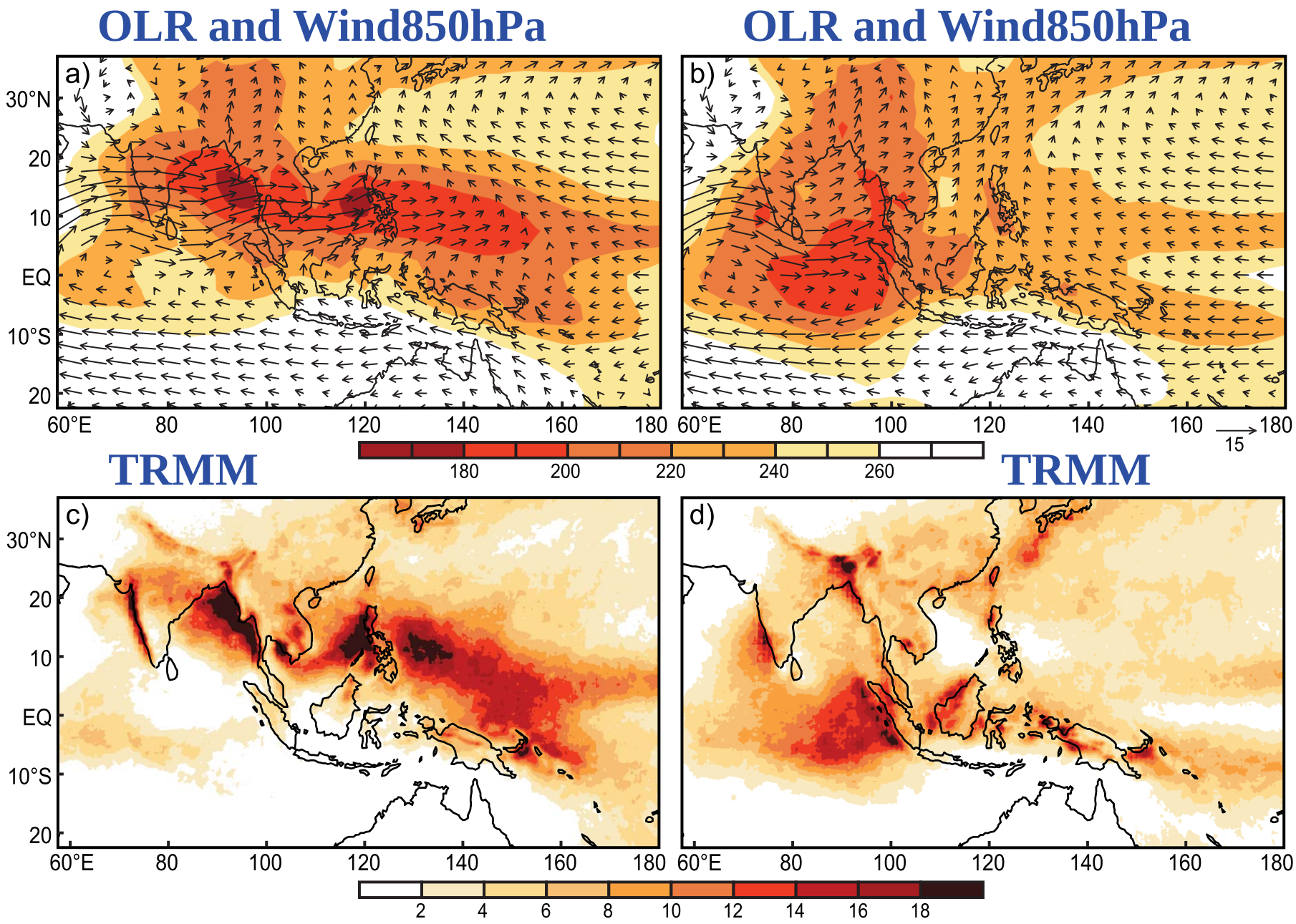
OLR and Wind850hPa
OLR and Wind850hPa
a)
b)
30°N
20
10
EQ
10°S
20
60°E
80
100
120
140
160
180
15
180
200
220
240
260
TRMM
TRMM
c)
d)
2
4
6
8
10
12
14
16
18

Active and break spells of the Indian summer monsoon rainfall

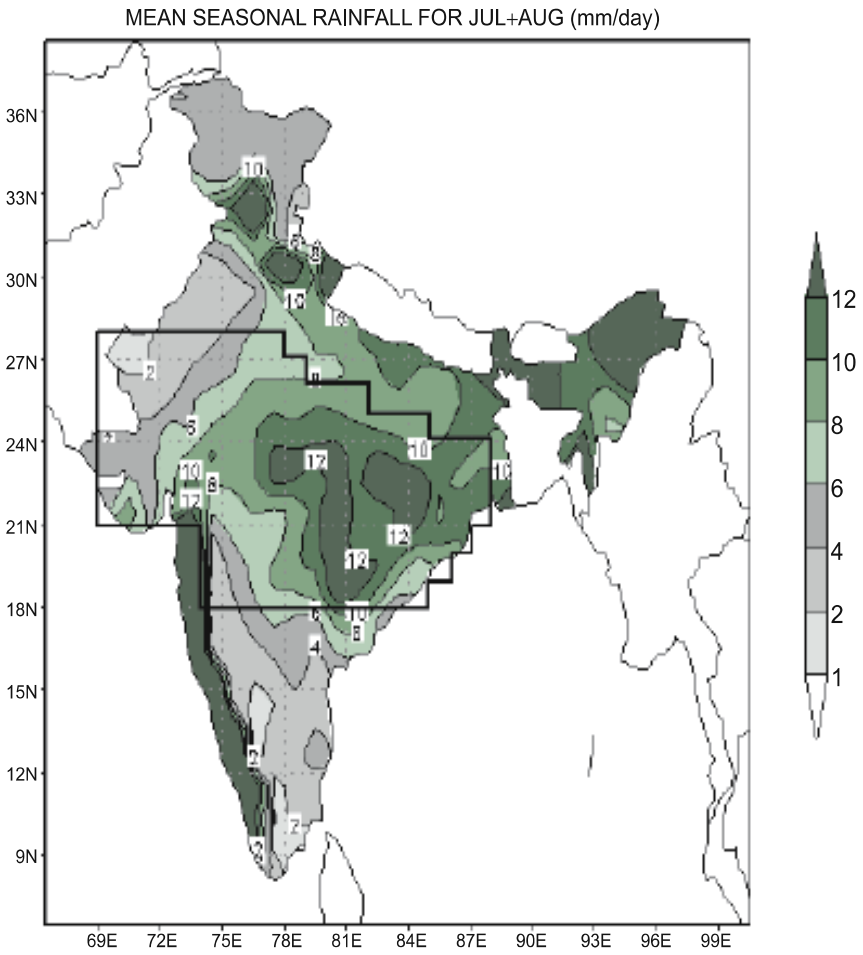

Active spell: **Standardized rainfall anomaly is less than -1.0, consecutively for three days and more**

Break spell: **Standardized rainfall anomaly is less than -1.0, consecutively for three days and more.**

Rajeevan, M., S. Gadgil, and J. Bhate, 2010: Active and break spells of the Indian summer monsoon. *Earth Syst. Sci.*, **119**, 229–247.

- Total number of active and break spell in **Rajeevan tables 1, 2** is 49 and 43 respectively in **July and August.**

- Total number of active and break spell in **this study** is 76 and 81 respectively in **June-July-August-September.**

- **10 active** spell and **5 break** spell is common in both study in **July-August (in out of 49 and 43 respectively).**

- This result is not good because correlation between PC1 of OLR (daily) and IMD rainfall is **very low (0.1).**

OLR regressed on standardized PC1 of JJAS pentad-mean (*a*) TRMM rainfall, (*b*) 850 hPa zonal wind, (*c*) 850 hPa vorticity, and (*d*) 150 hPa divergence.

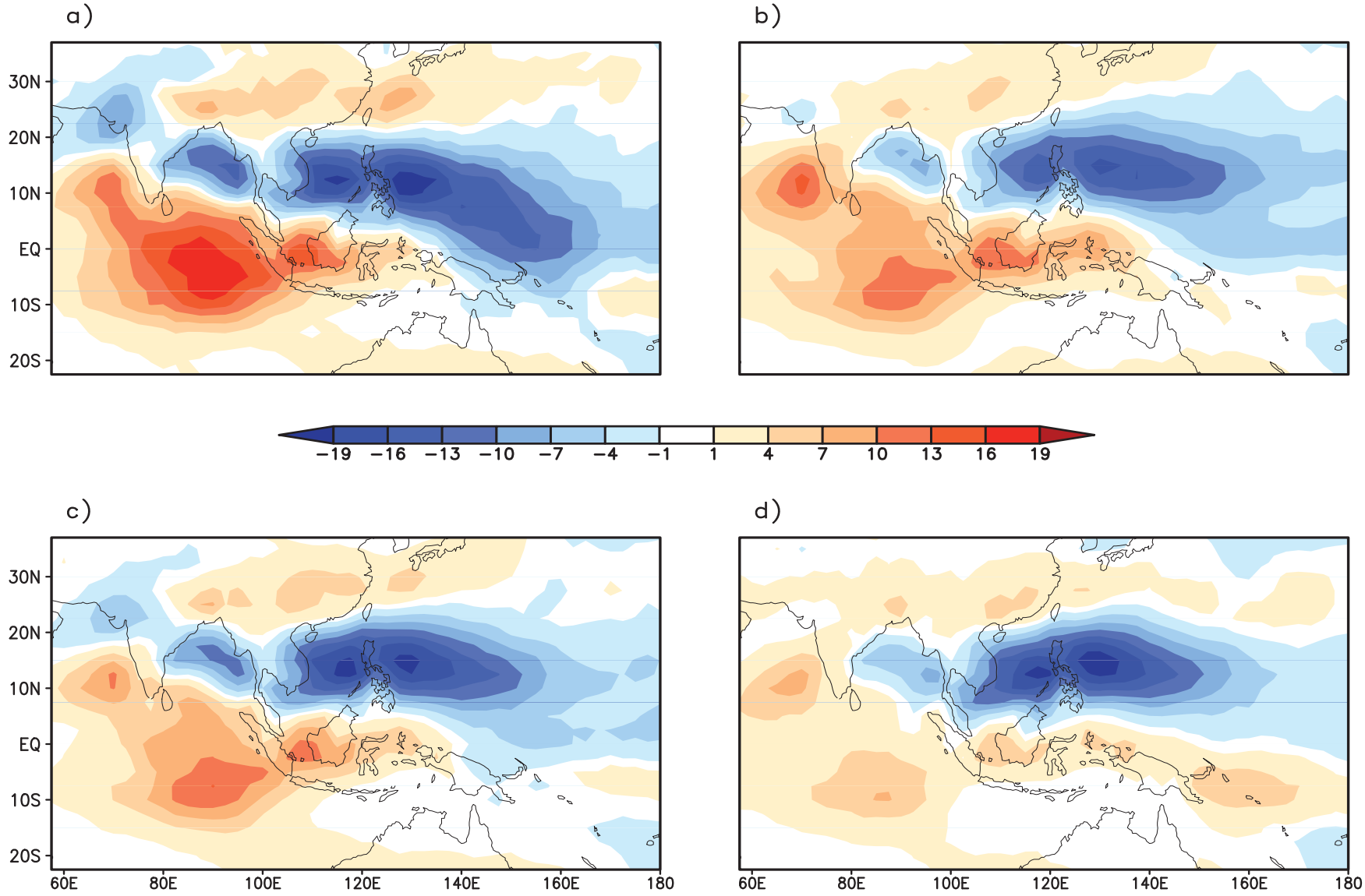

Matrix of correlation coefficients between the leading PC of different atmospheric variables, as indicated based on JJAS pentadal-mean

	OLR	850 hPa wind	850 hPa vorticity	150 hPa divergence	TRMM rainfall
OLR	1.00				
850 hPa wind	0.67	1.00			
850 hPa vorticity	0.73	0.89	1.00		
150 hPa divergence	0.50	0.66	0.68	1.00	
TRMM rainfall	0.92	0.73	0.83	0.63	1.00

Composite (*a*) OLR and (*c*) TRMM rainfall fields for days on which OLR averaged over the Bay of Bengal (12^{0}N to 18^{0}N, 83^{0}E to 92^{0}E) is less than 155 W m^{-2}. (*b, d*) As in (*a, c*) but for days on which TRMM rainfall averaged over the Bay of Bengal is greater than 23 mm d^{-1} (Algorithm similar to the one used by Bharatraj and Sengupta 2012)

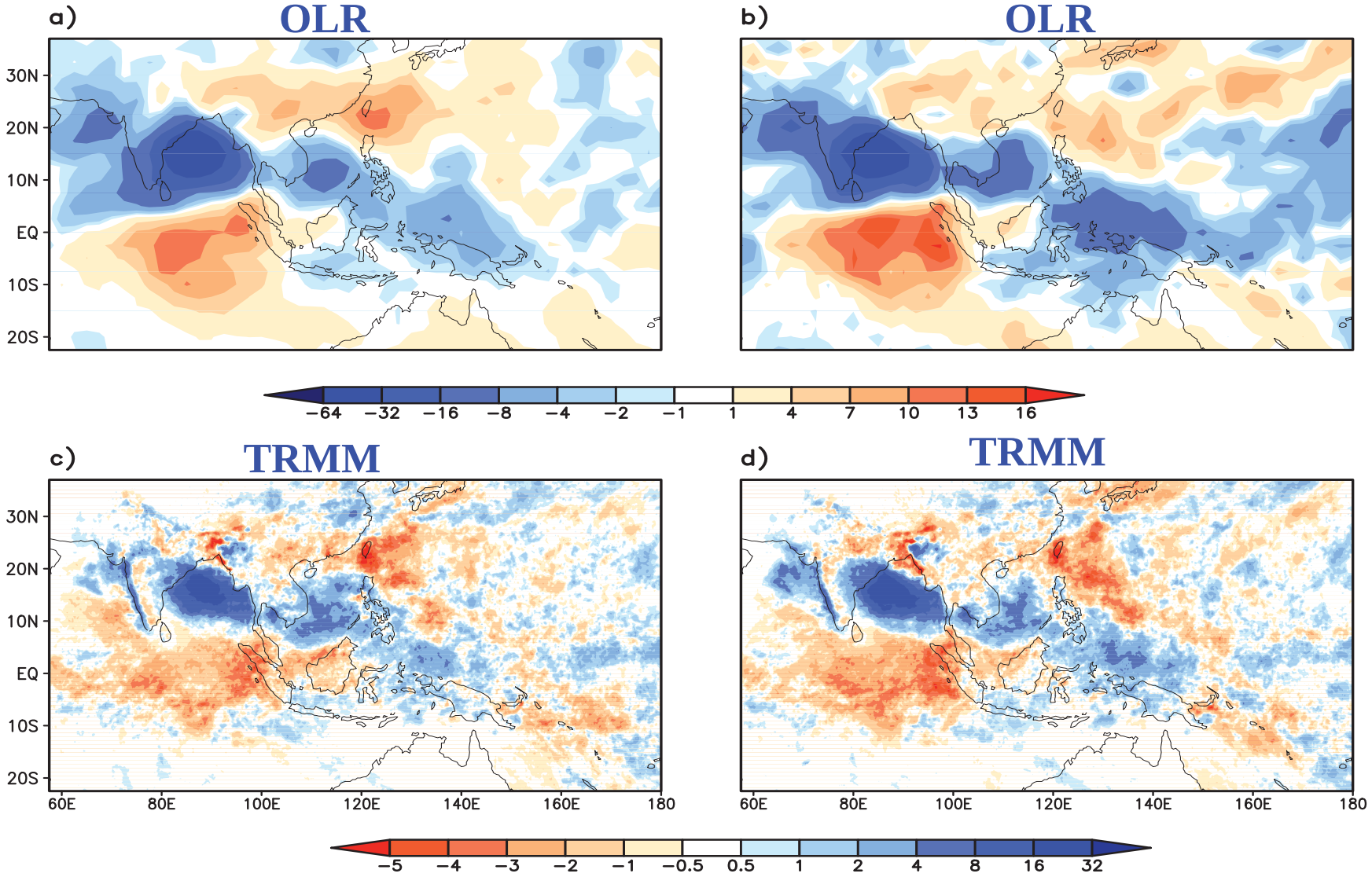

Thank You

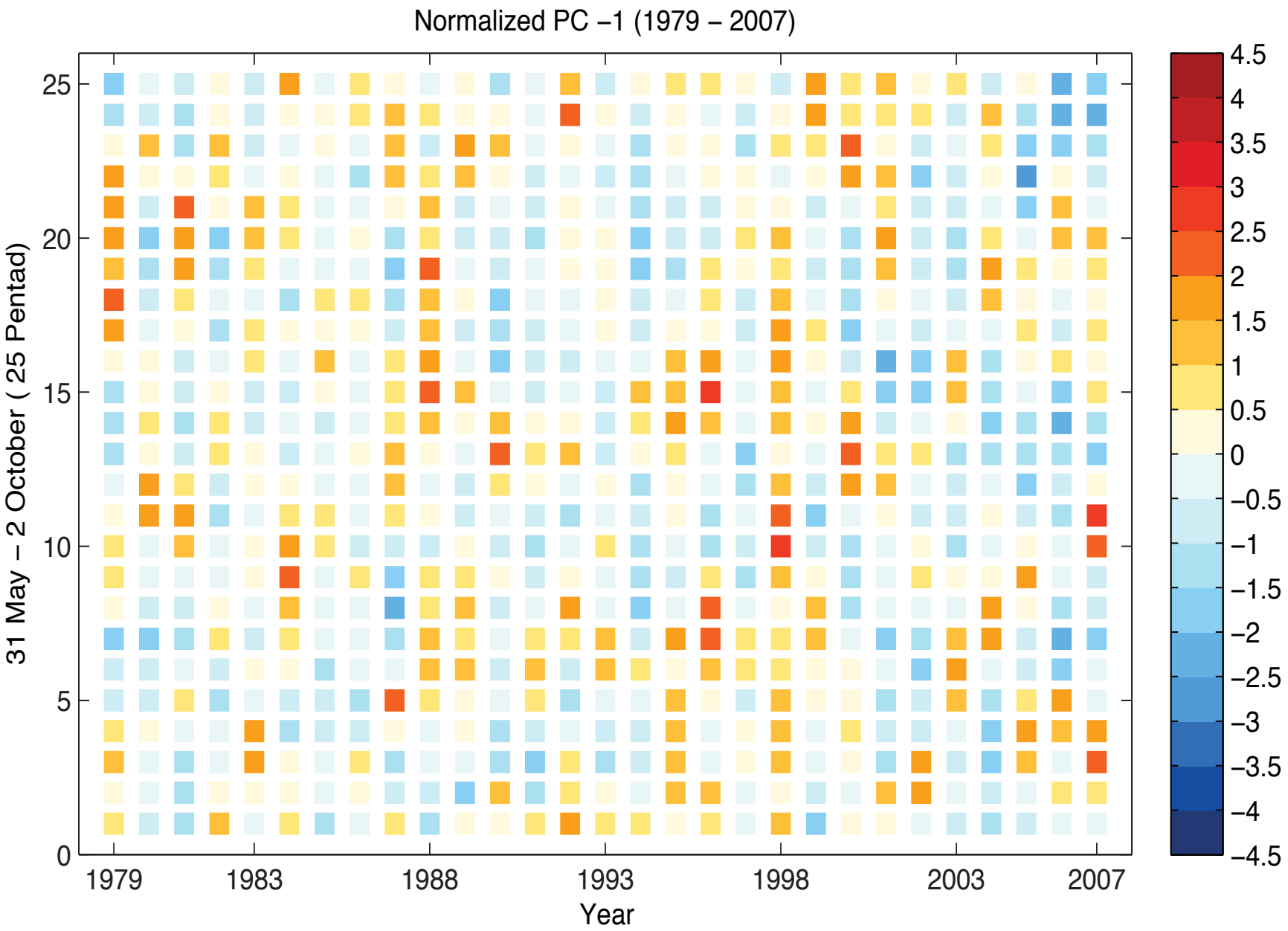
Normalized PC –1 (1979 – 2007)
31 May – 2 October (25 Pentad)
25
20
15
10
5
0
1979
1983
1988
1993
1998
2003
2007
Year
4.5
4
3.5
3
2.5
2
1.5
1
0.5
0
–0.5
–1
–1.5
–2
–2.5
–3
–3.5
–4
–4.5

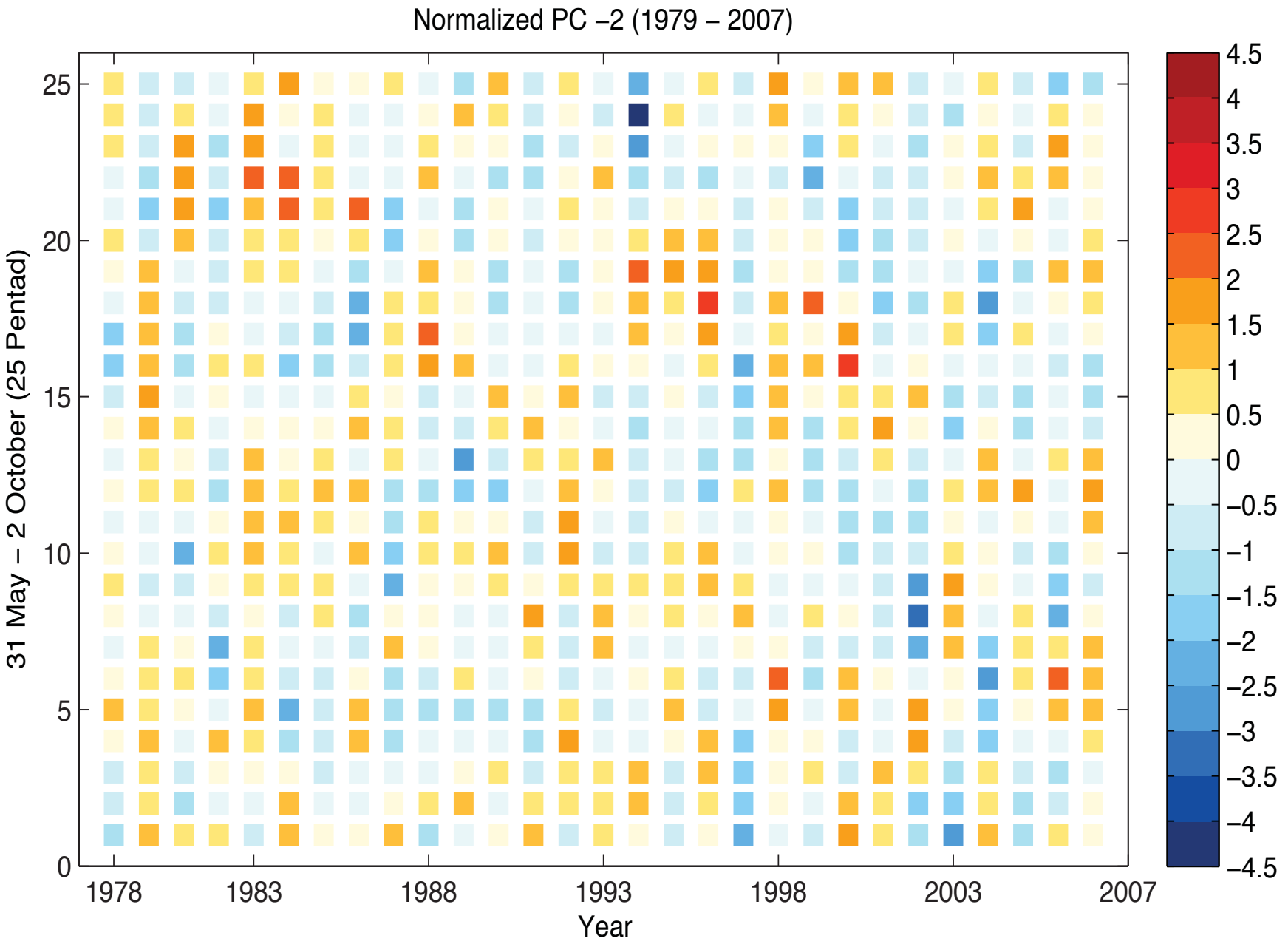
Normalized PC −2 (1979 – 2007)
31 May – 2 October (25 Pentad)
25
20
15
10
5
0
1978
1983
1988
1993
1998
2003
2007
Year
4.5
4
3.5
3
2.5
2
1.5
1
0.5
0
−0.5
−1
−1.5
−2
−2.5
−3
−3.5
−4
−4.5